scientific reports

Check for updates

OPEN

Traction force transmission via bioactive matrix hydrogel promotes epithelial collective migration mediated by integrin

Mingxing Ouyang[1,3]✉, Yu Cao[1,2,3], Hui Sheng[1,2], Hongjie Liu[1,2], Lei Liu[1], Chunmei Li[1], Bing Bu[1] & Linhong Deng[1]✉

Mechanical communications provide physical views to understand cell physiologies at large scale. Cell collective migration occurs often in vivo, of which the role of matrix tension force is largely unknown. Here to mimic in vivo conditions, we applied collective migration of renal epithelial MDCK cells on elastic matrix hydrogel containing bioactive materials of 50% Matrigel and 1 mg/mL type I collagen. MDCK cells were engineered with stable expression of ERK FRET (fluorescence energy resonance transfer) biosensor in regarding of ERK sensitivity in cell mechanical response. The results showed that matrix traction force derived from cells-generated contraction promoted epithelial sheet migration with higher ERK activity at the move front. Hydrogel crosslinking by glutaraldehyde blocked matrix traction transmission and then reduced ERK and epithelial collective migration. Integrin inhibition dramatically reduced collective migration but not local cell moving velocities, indicating integrin acting with mechanotransduction role at cells-hydrogel interface in orienting migration direction. Further experiments demonstrated that matrix traction force relied on activations of cellular mechanosensitive calcium channels, and ERK signal in promoting collective migration. In conclusion, matrix tension force derived from cell contractions facilitates epithelial collective migration through activating cellular mechanosensitive signals, in which integrin acts as mechanical transducer. This work highlights the role of matrix traction force in wound healing and tissue engineering.

Keywords Epithelial collective migration, Cell mechanical communications, Matrix traction force, Fluorescence resonance energy transfer (FRET), ERK, Integrin

Cell mechanical communications have been demonstrated with fundamental roles in regulating cell-cell distant interactions, tissue morphogenesis, developmental processes, immune cell responses, fibrosis, and cancerous migrations[1–7]. It provides a physical pathway to understand the cell physiologies at large scale besides the biochemical signaling. The mechanical communications underlie several special features including active contraction forces generated by cells, the merging and long directional transmission of contractive forces in the matrix microenvironment, cell high mechanosensation, and the extracellular matrix remodeling by active traction forces[8–12]. Collective cell migration plays an important role in a series of biological processes such as embryonic development, immune response, cancer metastasis and wound healing[13,14]. It is still largely unknown whether and how cell mechanical communications promote the collective migration processes through traction force transmission via the extracellular matrix.

Cell collective migration is a usual phenomenon driven by both chemical and biomechanical factors like epithelial sheet migrations, and neural crest migrations[15–18]. In Drosophila embryonic development, cells migrate in groups to build different tissues or organs in the body[19]. In Xenopus, the cell mass of neuronal ridge moves to the destination collectively, and the upward contraction of the cells at the back assists the directed migration[20–22]. Wound healing experiments based on mechanical, chemical, optical and electrical methods have been developed to study the collective migration processes of monolayer cells[23,24]. By single-cell level analysis, the main drivers of migration are the extension of the frontal lamellar prominences, the establishment of new

[1]Institute of Biomedical Engineering and Health Sciences, School of Medical and Health Engineering, Changzhou University, 1 Gehu Rd, Wujin District, Changzhou 213164, Jiangsu Province, China. [2]School of Pharmacy, Changzhou University, Changzhou 213164, Jiangsu Province, China. [3]Mingxing Ouyang and Yu Cao contributed equally to this work. ✉email: mxouyang@cczu.edu.cn; dlh@cczu.edu.cn

adhesion sites at the front, cell body contraction, and the detachment at the back of the cell[25,26]. MDCK cells have clear apical-basolateral polarity and cell tight connections and are often used as models for collective epithelial migration[27–30].

As one research area to clarify the physical principles in life sciences, mechanobiology has grown into an important field of biomedical research, especially at the microscopic level of cells and molecules[31,32]. Long-range intercellular force transmission through cell-cell junctions on polydimethylsiloxane (PDMS) gels promotes epithelial layer migration direction by activating ERK signal wave[33,34]. The neural crest cell group migrates collectively in a supracellular manner, having a continuous contractility behind the cell cluster, and generating its own stiffness gradient within the body tissue[35,36]. Studies have shown that collective cell migration requires mechanical coordination between neighboring cells, and that mechanical forces can be transmitted via cell-cell contact from the leader cell at the edge of the migratory colony to the follower cell at the center[37]. However, the contributive role of tension force transmission via the underlying matrix hasn't been well studied during cell collective migration processes.

Cells can interact with each other through mechanotransduction to coordinate their movements in collective migration. Extracellular matrix (ECM) molecules interact with receptors on the cell surface to trigger intracellular signaling pathways[38–40]. Integrin is a such group of mechanosensitive transmembrane receptors to regulate persistent cell migration and cancer invasion[22,41]. By sensing and responding to mechanical forces, Piezo1 triggers calcium ion signals in cells, and knockdown of Piezo1 limits the increase in migration and proliferation of gastric cancer and ovarian cells[42–44]. Our work has also demonstrated the necessities of integrin and Piezo signals, actomyosin contraction, ER calcium channels, and cell junctional complex in cell distant mechanical interactions[45,46].

The extracellular signal-regulating kinase (ERK) shows high sensitivity to cell mechanical signals[47,48]. The ERK signaling pathway consists of core protein kinases Raf, MEK, and ERK1/2, which regulates various biological outcomes such as cell proliferation, differentiation, and cell migration[49,50]. ERK1/2 are transferred to the nucleus after activation, and regulate the activity of various transcription factors through phosphorylation[51,52]. The fluorescence resonance energy transfer (FRET)-based EKAREV-NLS biosensor (nuclear ERK FRET) converts ERK activity into FRET signal changes through reversible phosphorylation of ERK substrate peptide which is derived from Cdc25c for Pin1 WW domain binding[50,53]. During cell collective migration, the FRET-monitored ERK activation waves repeatedly propagate from leader cells to follower cells[54,55]. This ERK activation wave, combined with mechanical force generation and pre- and post-cell polarity, results in coordinated cell migration over long distances[34,37,56]. In this work, we generated MDCK cell line stably expressing EKAREV-NLS biosensor to monitor matrix tension force-regulated ERK activity during collective migration.

An important question to be addressed in this study is the role of long-range force transmission via the ECM matrix in cell collective migration. The experimental design was to monitor the migration of MDCK epithelial monolayer seeding on nonlinear elastic matrix hydrogel, which was different from hard substrate not allowing force propagation. By combining with ERK FRET measurements, our work demonstrated that traction force transmission via the matrix hydrogel promoted epithelial collective migration, which relied on ERK activity, cell contraction and calcium channels and Piezo1 mechanosensations. Interestingly, integrin regulated the epithelial migration direction, likely by mediating the force transmission between cells and ECM matrix. As a work model, epithelial cells-generated contractions are transmitted and merged as traction forces in the matrix hydrogel, which feedback facilitates epithelial collective migration.

Materials and methods

Cell culture and reagents

Madin-Darby canine kidney (MDCK) cells were purchased from Beina Science & Technology Company, Shanghai. The cells were cultured in high-glucose DMEM medium supplemented with 10% fetal bovine serum (FBS) in a humidified incubator containing 5% CO_2 at 37℃. After grown into confluence, the cells were sub-cultured by passaging or taken for experiments at the logarithmic-growth phase.

High-glucose DMEM, Opti-MEM medium, fetal bovine serum, Lipofectamine 3000 were purchased from Thermo Fisher Scientific, Massachusetts. Matrigel was purchased from BD Biotechnology, and type I collagen from Advanced Biomatrix. The inhibitors purchased from MedChemExpress (MCE) included Y27632 (ROCK inhibitor, 40 μM as applying concentration), Thapsigargin (10 μM), GsMTx4 (5 μM), $GdCl_3$ (calcium-sensing receptor agonist, 25 μM), and PD98059 (MEK inhibitor, 10 μM). Amino-ethoxydiphenyl borate (2-APB, 10 μM), Nifedipine (10 μM), Blebbistatin (40 μM), and ML-7 (40 μM) were ordered from Sigma. A Ⅱ B2 antibody (2 μg/mL) was ordered from Developmental Studies Hybridoma Bank (DSHB).

Establishment of stable ERK-FRET MDCK cell lines

To elucidate the mechanical signaling mechanisms underlying epithelial sheet migration, we introduced cell nucleus-located ERK FRET biosensor EKAREV into MDCK cells and generated stable-expression cell line. Specifically, the EKAREV expression plasmid was transfected into MDCK cells with Lipofectamine 3000 reagent. After 48 h, G418 antibiotics was added at a concentration of 300 μg/mL to select positively transfected cells. The medium containing G418 was changed every three days. Two weeks later, the cells that grew into fluorescent clusters were further diluted into 96-well plate at low density for monoclonal culture. The cell colonies showing 100% fluorescence were screened and selected under the microscope, followed by culture amplification to establish the stable ERK-FRET MDCK cell lines.

Preparation of hydrogel in the polydimethylsiloxane (PDMS) mold, and collective migration model of MDCK cells

The preparation of PDMS mold was introduced in our previous work[57]. In brief procedures, the PDMS base and the crosslinker (Sylgard 184 kit, Dow Corning) were fully mixed at a mass ratio of 10:1, and cured at 70℃ for 4 h. The PDMS circular chamber by drilling a hole in 1.0 cm diameter was plasma-treated, ultrasonic-cleaned, soaked in 70% alcohol, and then affixed onto the glass bottom of confocal dish to assemble the PDMS mold. Before experiments, the mold was filled with hydrogel solution (50% Matrigel, or 50% Matrigel containing 1 mg/mL COL) and left at 37 ℃ for 15 min. To create the condition for directional epithelial-sheet migration, a cubic stand of 4% agarose gel in a size of 0.5 × 0.5 cm square section was placed at the central area of the hydrogel surface, and MDCK cells (7×10^3 cells/cm^2) were inoculated on the rest area of hydrogel surface. After cultured for 24 h when the cells grew into 100% confluency, the agarose gel stand was removed gently, and then cell monolayer migration was imaged under FRET microscopy.

As a negative control without matrix force transmission, the hydrogel was crosslinked with 0.05% glutaraldehyde solution for 15 min, followed by thrice phosphate buffered saline (PBS) washes, and neutralization with 50 mM Tris-HCl (PH 7.0) for 1 h. As control experiments on hard surface, the confocal dishes were coated with diluted ECM molecules (2% in mass concentration) for MDCK cells collective migration. First, 500 μL of adhesive ECM solution containing 2% Matrigel+collagen, 2% Matrigel only, or 2% collagen only was spread on glass-bottom surface of the confocal dish and incubated at 4℃ overnight. On the second day, the solution liquid was sucked out, and 4% agarose gel blocker was placed on the center of glass-bottom surface, followed by the similar procedures with MDCK cells seeding and FRET imaging.

To determine the mechanical properties of the hydrogels under the different conditions, we measured the elasticity and viscosity by a rotational rheometer (Kinexus, Malvern), which probe covered 2 cm of the circular hydrogel surfaces in diameter. The procedures were described in details in the recent lab work[58].

Beads-tracking measurement of matrix hydrogel deformation during cell monolayer migration

Black magnetic beads (0.48 μm in diameter) were mixed into the hydrogel at 1/250 volume ratio. Since the beads did not have fluorescence, cell migration was photographed at an interval of 30 min using the microscopic brightfield mode for 10 h. The deformation of the hydrogel during MDCK cells collective migration was determined by the position shifts of magnetic beads, which indicates the relative comparisons of local traction forces in the hydrogel.

Time-lapse FRET microscopic imaging

As described in our previous work, the epi-microscopy system (Zeiss) was equipped with the X-Y-Z control stage for multi-position function, fine auto-focusing for time-lapse imaging, and temperature-CO_2 (37℃-5%) chamber to maintain cell culture conditions. During FRET image acquisitions through ECFP and FRET (YPet) channels, the parameters for excitation filter and dichroic mirror were 436 ± 10 nm and 455 nm, respectively, and the emission filters of ECFP and FRET (YPet) channels were 475 ± 20 nm and 535 ± 15 nm, respectively. The FRET imaging on hydrogel was visualized with ×20 objective at an interval of 15 min for 10 h. The ECFP and FRET channels were swiftly switched automatically as controlled by Zeiss software during the real-time acquisition of dual-channel images.

FRET image quantifications, trajectory analysis of cell movements, and beads tracking assay in hydrogel

The Graphpad Prism 6 software was used to complete data processing and statistical analysis. 20–30 leading cells (front group) or following cells of epithelial sheet migration (back group), which stably expressed nuclear ERK FRET biosensor, were manually circled to measure their FRET ratiometric values. The FRET image analysis software Fluocell 6.0.0 (Lu S et al., USA) was used for data analysis[59]. After subtraction of background noise, the fluorescence signals of ECFP and FRET images were measured, and the ratio of the two channels was calibrated in spatial pixel-to-pixel manner. Quantitative FRET data were expressed as scatter points in graphics (mean ± S.D.).

ImageJ software was used to process trajectory analysis of time-course cell images, and the spatial distance in pixels was converted into length in μm on the images by the "Set Scale" function. "Manual tracking" function from the plugin list (Plugins→ Tracking→ Manual tracking→ Add track) was applied to track the movement displacements and distances of individual cells at the front group. The data in the Result window was saved as Excel file. The speed of cell movement was calculated via the displacement divided by migrating time, and the velocity via the distance divided by the time. The data was expressed as scatter points in graphics as mean ± S.D.

Graphpad Prism 6 software was also used to compare the statistical difference between the control group and the experimental groups, and multiple T-test analyses were performed according to different experimental conditions. *, **, *** and **** indicate p values < 0.05, 0.01, 0.001, and 0.0001 for significant differences, respectively.

Results

The traction force transmitted over matrix hydrogel influences MDCK cells collective migration and ERK activation

MDCK cells are a common experimental model for studying collective migration, tubulogenesis, and tight junctions[60]. Here, the cell line with stable expression of ERK FRET biosensor was generated to visualize cell directed migration in monolayer and mechanosensitive ERK activity. To create different conditions for traction force transmission efficiencies, three types of matrix hydrogels were applied in the study, including Matrigel

containing 1 mg/mL type I collagen (Mat + COL), Matrigel only (only Mat), and cross-linked Mat + COL with glutaraldehyde (Gluta-fixed Mat + COL). As shown in our previous work, the fixed Mat + COL hydrogel had nearly no traction force transmission as negative control[57]. After the hydrogel was prepared within the circled PDMS mold, a cubic blocker of 4% agarose gel was placed on the center, followed by seeding MDCK cells on top of the rest hydrogel area. After 24 h, the cells grew into confluency to create a monolayer directional migration model, and time-lapse FRET imaging was performed at interval of 15 min for 10 h.

As shown by ERK FRET images, MDCK cells seeding on the matrix hydrogels displayed monolayer collective and directional migrations towards the blank hydrogel surfaces (Fig. 1A, Movie 1). This indicates that the experimental model for epithelial collective migration worked well on the matrix hydrogels. FRET quantification at the 10th h timepoint showed higher ERK activity at the migration front groups than at the back groups, whereas that difference was less obvious on Gluta-fixed hydrogel (Fig. 1B). By comparing the FRET levels on three types of hydrogel conditions, ERK activity was higher at the front of Mat + COL group than that of only Mat or Gluta-fixed group, and also certain higher than only Mat one for the back groups (Fig. 1C). Migration quantification of MDCK monolayers demonstrated that the move speed was more than 100% faster on Mat + COL than the other two conditions (Fig. 1D). Trajectory analysis of individual cells at the migration fronts also showed much quicker movements for the Mat + COL group than the other two groups (Fig. 1E). Hence, the mechanosensitive ERK activity was in consistent trend with the monolayer migration speed, which suggests higher tension force on the Mat + COL hydrogel.

To further demonstrate traction force transmissions via the matrix hydrogels during MDCK monolayer migrations, black magnetic beads (4.82 μm in diameter) were embedded into the hydrogels, which position shifts helped reflect the relative traction force magnitudes. As shown by time-lapse brightfield imaging, the beads visible on the hydrogel surfaces moved forward at slower pace along with the epithelial layer, but not obviously on the Gluta-fixed one (Fig. 2A). Quantified by trajectory analysis and move velocities, the beads from Mat + COL group moved 50% faster than those from only Mat one at average in the 10 h, and beads from Gluta-fixed group had almost no position shift forwards (Fig. 2B). These results indicate that there was traction force transmission via the matrix hydrogel during the MDCK monolayer migration, and the traction force looked higher on Mat + COL than only Mat, and almost no traction transmission happened on Gluta-fixed one. The comparisons in traction force difference are consistent with the monolayer moving speeds and ERK activities.

To more precisely determine the mechanical properties of the hydrogels during the revision, we measured the elasticity and viscosity by a rotational rheometer (Kinexus, Malvern). As the results shown in Fig. 2C, the viscosities of the four types of hydrogel conditions had little difference, whereas glutaraldehyde-crosslinking made the elasticity more dominant with an increase from ~3 Pa at normal condition to ~8 Pa at fixation. Matrigel only had a little lower elasticity than Mat + COL one, and addition of 4.8 μm beads (1/250 volumetric ratio) didn't change the elasticity.

We also examined the coated glass surfaces with diluted ECM molecules (2% in mass concentration), which could maintain the integrin signaling but without traction force transmission via the hydrogel. As shown in Supplementary Fig. S1A, MDCK cells had collective migrations on the coated surfaces. FRET quantifications didn't show much difference in ERK activities between Mat + COL and only Mat coatings, while COL only coating had more stimulation on ERK activation (Supplementary Fig. S1B), maybe due to more integrin activation by the relatively higher COL coating density (i.e. 2% COL in solution). From migration quantifications, the moving speeds/velocities of individual cells didn't show much difference on the three coating conditions, although COL only one had slight increase in speed (Supplementary Fig. S1C-E). Taken together with the results from Gluta-fixed hydrogel, traction transmission via the matrix hydrogel played important role in promoting the epithelial monolayer migration, although the ECM structure self is necessary in integrin activation and collective migration.

Matrix traction-promoted epithelial monolayer migration relying on ERK, cell contraction force, and calcium channels activation

ERK activity showed consistency with the traction force and collective migration rate on the different hydrogels. We tried to confirm whether ERK regulates the migration. Treatment with ERK inhibitor PD98059 significantly reduced ERK FRET levels on Mat + COL hydrogel (Fig. 3A&B), which also resulted in remarkable reduction of MDCK monolayer migration (Fig. 3C&D). This result is consistent with the previous report for ERK role in collective migration[37]. In considering the reduced ERK activity and migration on Gluta-fixed hydrogel (Fig. 1A-C), these data together suggest ERK activation by the matrix traction force, which then promotes the epithelial migration.

We hypothesized that the traction force transmitted via the matrix hydrogel was originated from cells-generated contractions. The data in Fig. 2 demonstrated traction force transmission by beads tracking assay, hence we further tested the importance of cell contraction force in this model. Myosin family are the major contractive force generators on actin filaments, regulated by Rho-ROCK signaling. We applied ROCK inhibitor Y27632, myosin II ATPase inhibitor Blebbistatin, and myosin II light-chain kinase (MLCK) inhibitor ML-7 in the epithelial monolayer migration seeded on Mat + COL hydrogel (Fig. 4A). In quantitative comparison to the control group (DMSO), ERK activity was apparently down-regulated by treatments with the three inhibitors (Fig. 4B). This result also supports the contribution of matrix traction force to ERK activation. Migration quantification demonstrated remarkable reduction in moving rates by the three inhibitors during MDCK monolayer migrations (Fig. 4C-D). The results are consistent with matrix traction force being derived from cell contractions in promoting the collective migration. As the cell contraction inhibitors could have broad effects on cell physiologies, particularly under the long-term experimental incubation (~10 h), the specific impact on matrix traction force need be further clarified from the general cellular changes by the contraction inhibitors.

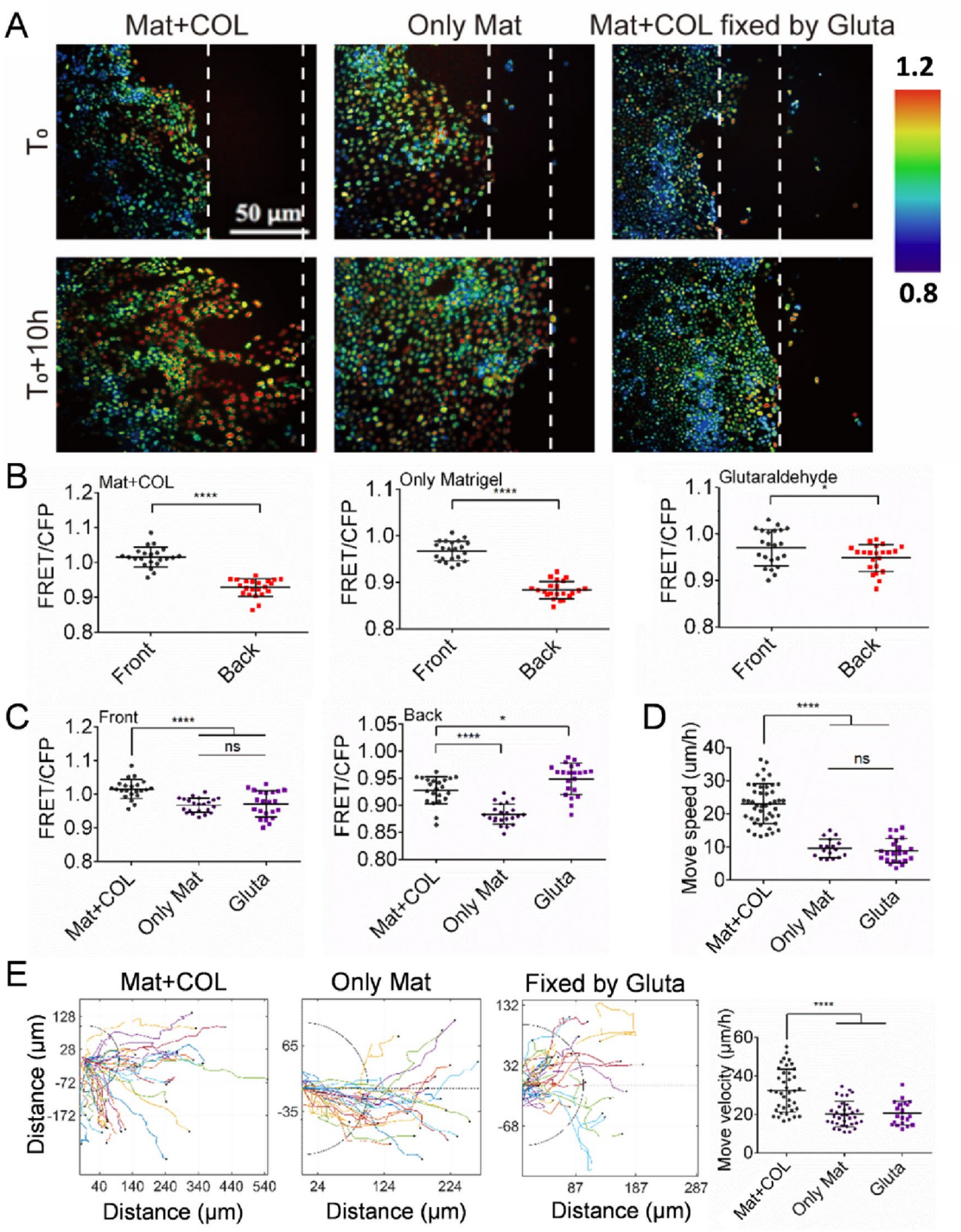

Fig. 1. The influence of matrix traction forces on MDCK epithelial collective migrations on three types of matrix hydrogels by ERK FRET imaging. The imaging was done simultaneously for the three types of hydrogel conditions under the same experimental set while combined of independent repeats. **(A)** ERK FRET (YPet/ECFP) ratiometric imaging of cell monolayer migrations on Mat + COL hydrogel, only Mat, and cross-linked Mat + COL by glutaraldehyde (Gluta fixation). The representative images display the beginning and 10th h timepoints along with the white lines roughly indicating the migration front changes; the pseudo-color scale bar indicates FRET ratio values from high (red) to low (blue). **(B)** Comparisons of ERK FRET ratio at the front or back cell groups at 10th h timepoints (mean ± S.D., $n = 30$), respectively. **(C)** FRET comparisons of the front or back cell groups on the three types of hydrogel conditions ($n = 30$). **(D)** Quantitative comparison for moving speeds of individual cells at the front groups (μm/h) within 10 h. The sample size $n = 39, 17, 23$, respectively. **(E)** Trajectory analysis of individual cells from the migration front groups and their moving rate comparison in 10 h ($n = 35, 39, 20$). The diameter of the shown trajectory circles is 100 μm. In statistical analysis by T-test, *, **, ***, **** indicate $P < 0.05, 0.01, 0.001, 0.0001$ for significant differences, respectively, and so on through the article.

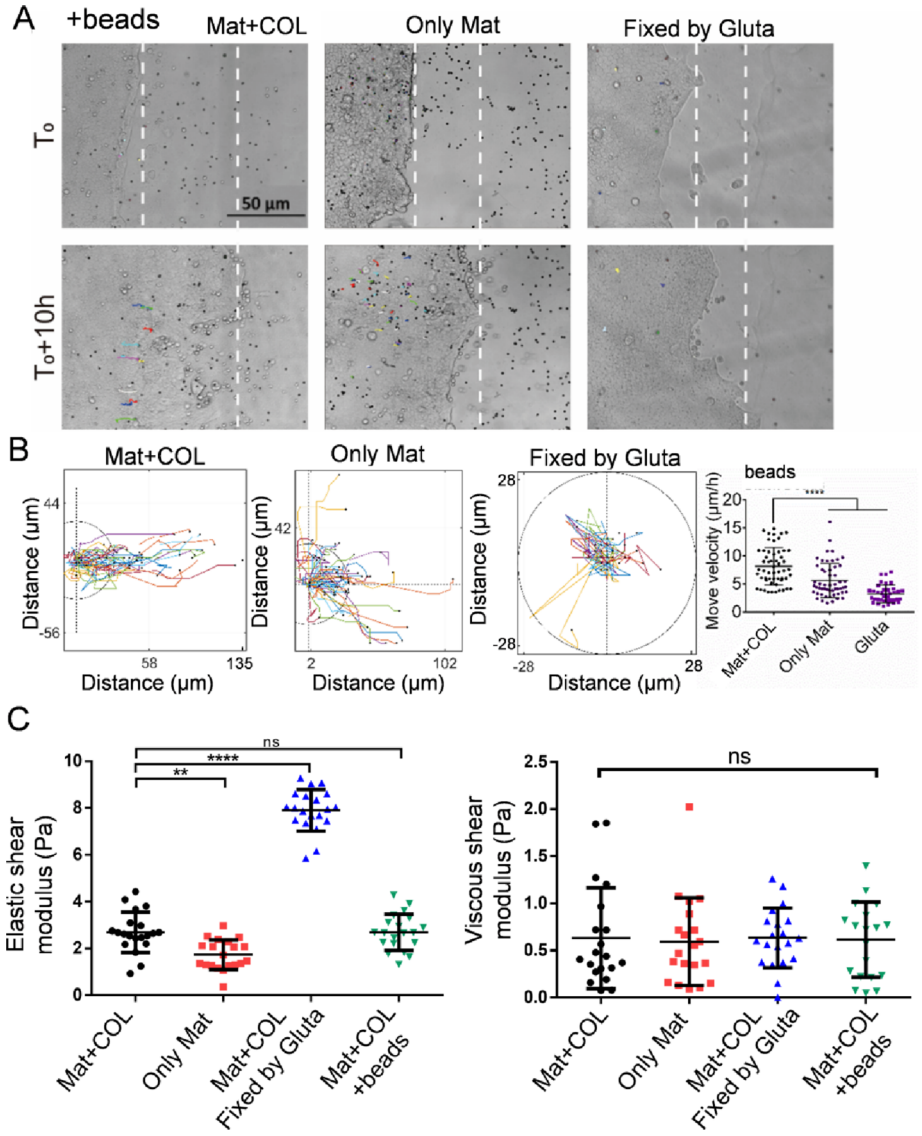

Fig. 2. Demonstration of traction forces in the hydrogels by beads tracking assay. MDCK cells were seeded on the three types of hydrogel conditions embedded with 4.82 μm black magnetic beads. **(A)** Time-lapse brightfield imaging of cell monolayer migrations in 10 h with black magnetic beads embedded in the hydrogels. **(B)** Trajectory analysis of individual beads and moving rate comparison at the migration front groups in 10 h ($n = 55, 37, 57$). The diameter of the shown circles is 30 μm.

Cellular calcium signals are sensitive to mechanical stimulus[61], and our previous work also identified substrate stretch-induced ERK activation through calcium channels mechanosensation[48]. To further demonstrate the role of calcium signals in the traction force-promoted epithelial migration, inhibitors for different calcium channels were applied in the model including $LaCl_3$ (a non-permeable inorganic compound blocking bivalent cation channels on plasma membrane), 2-APB (selective ER IP_3R Ca^{2+} channel inhibitor), Nifedipine (inhibiting L-type Ca^{2+} channel on plasma membrane), and Thapsigargin (selective ER SERCA calcium pump inhibitor) (Supplementary Fig. S2A). FRET quantifications showed that ERK activities were apparently reduced by these inhibitors, while with less impact from $LaCl_3$ (Supplementary Fig. S2B). Migration quantification also demonstrated remarkable decreases in MDCK collective migrations under coculturing with these inhibitors, except $LaCl_3$ with less obvious inhibitory role (Supplementary Fig. S2C-D). These data indicate that the calcium channels on plasma membrane and endoplasmic reticulum are important for ERK activation and monolayer migration on Mat + COL hydrogel, which implicates a connective signaling role in matrix traction-induced mechanotransduction.

Integrin mediates epithelial migration direction on matrix hydrogel along with indispensable role from Piezo1

Integrins are dimers composed of subunits α and β in transducing the inside-out and outside-in biomechanical signals between cell membrane and extracellular matrix[62]. To verify the role of integrin in mechanosensing

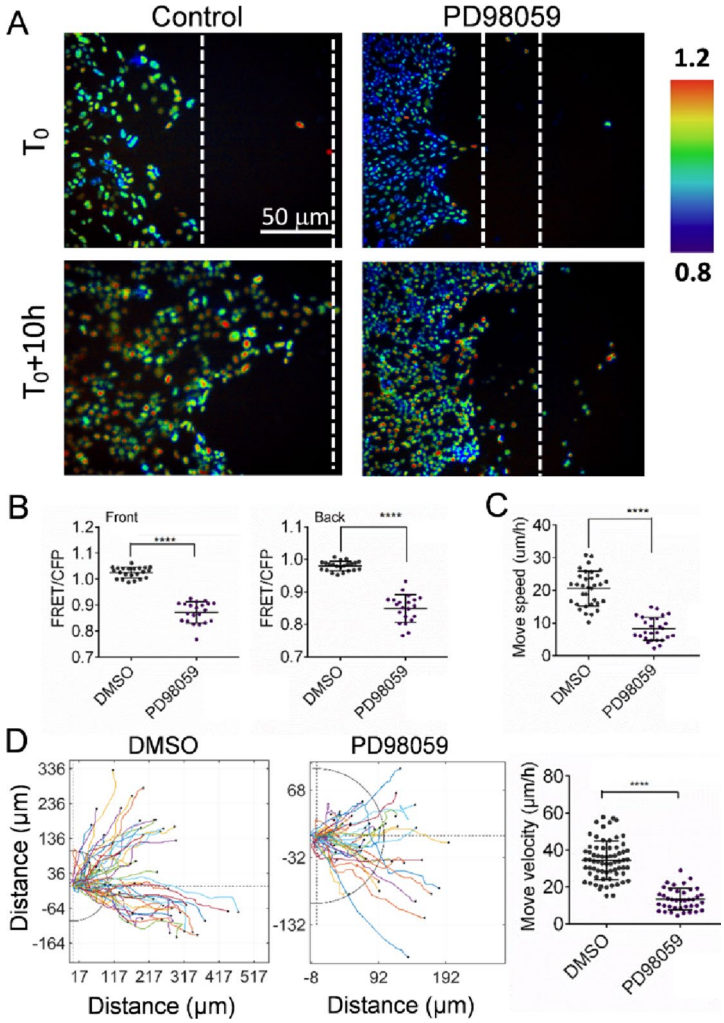

Fig. 3. Effect of ERK activity on MDCK collective migration. MDCK cells were seeded on Mat + COL hydrogel cocultured with DMSO or ERK inhibitor PD98059. **(A, B)** ERK FRET ratiometric images (A), and FRET comparisons of the front and back cell groups (B, $n = 30$) for cell collective migrations under the indicated conditions. **(C)** FRET comparisons of the front or back cell groups between control DMSO and PD98059 treatment ($n = 30$). **(D, E)** Quantitative comparisons of moving speed (D, $n = 33, 31$)) and trajectory analysis of individual cells (E) from the migration front groups in 10 h ($n = 40, 65$).

matrix traction force during the epithelial migration, inhibitory AIIB2 antibody for integrin β1 was cocultured in the experimental model, along with a positive control $MnCl_2$ which Mn^{2+} can activate integrin binding to its ligand on cell surface[63] (Fig. 5A). In comparison to the control group, AIIB2 inhibited ERK activity while Mn^{2+} enhanced it (Fig. 5B). Surprisingly, inhibition of integrin activity by AIIB2 antibody suppressed the epithelial collective migration, but had almost no inhibitory role in the moving velocity of individual cells (Fig. 5C). From trajectory analysis, AIIB2 treatment caused cells losing forward-moving direction, but not local moving velocity (Fig. 5D), as also seen obviously in the time-lapse Movie 2. The results indicate that matrix traction force-promoted epithelial migration required appropriate mechanotransduction by integrin signals to move forward. $MnCl_2$ treatment had slight inhibition on the epithelial migration speed, but not on the moving velocity (Fig. 5C-D). However, $MnCl_2$ had side-effect on cell viability (Fig. 5E), which complicated the interpretation during the 10 h imaging process.

Piezo1 channel helps cells sensing the environmental mechanical stimulus[64]. Hence, we also tested the role of Piezo1 in the traction force mechanotransduction by coculturing with Piezo1 activator YODA1, or two inhibitors GsMTx4 and $GdCl_3$ (Fig. 6A). From migration analysis, GsMTx4 and $GdCl_3$ remarkably reduced epithelial migration and cell moving velocity, while YODA1 didn't show obvious impact (Fig. 6B-D). Along with the results in Fig. S2A-D, the data support the role for mechanosensitive calcium channels (including Piezo1) in the epithelial migration. GsMTx4 and $GdCl_3$ were not specific inhibitors for Piezo channels only, and constant activation of Piezo1 by YODA1 may have complicated impact on cell physiology. Hence, these results provide only supportive evidence for interpreting Piezo1 role in traction force-promoted collective migration.

In considering of matrix traction force derived from cell contractions, we further checked the traction changes by beads tracking assays under integrin β1 inhibitor AIIB2 antibody or Piezo1 inhibitors GsMTx4

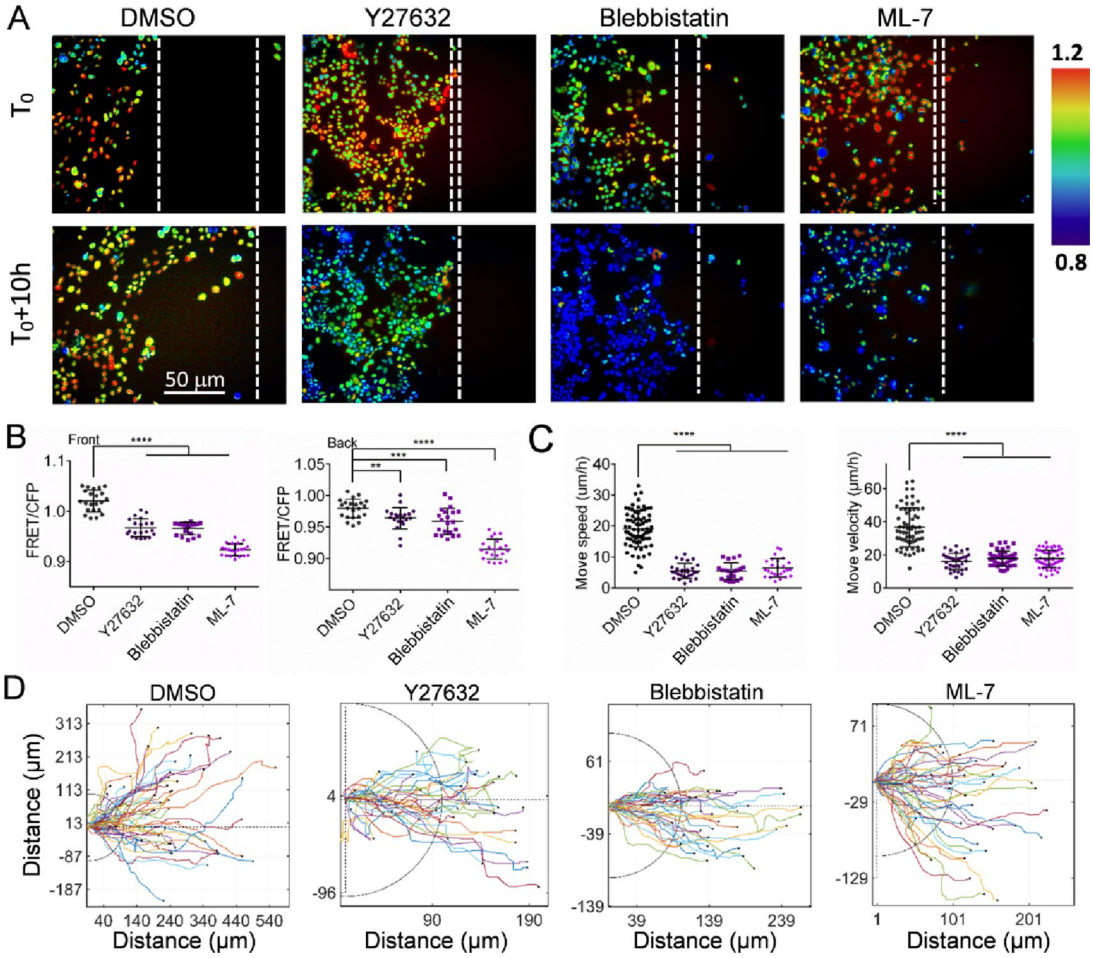

Fig. 4. Cell contraction force in regulating epithelial cell migration. MDCK cells were seeded on Mat + COL hydrogel incubated with cell contractility inhibitors, followed by immediate time-lapse imaging. **(A)** Representative ERK FRET images during collective migrations with or without the indicated inhibitor (Y27632, Blebbistatin, ML-7). **(B)** FRET level comparisons of the front or back cell groups ($n = 30$) between control (DMSO) and inhibitor treatments at the 10th hour timepoint. **(C)** Quantitative comparisons of cell moving speeds and velocities between control (DMSO) and inhibitor treatments. The sample size $n = 73$, 35, 35, 21 (speed), and 69, 36, 43, 60 (velocity), respectively. **(D)** Trajectory analysis of individual cells from the migration front groups in 10 h under the indicated conditions.

and $GdCl_3$ (Fig. 6E). In comparison to the control, either integrin or Piezo1 inhibition dramatically reduced matrix tension force, as shown by beads trajectory analysis and moving velocities (Fig. 6F). Regarding that AIIB2 inhibited beads velocity but not cell velocity (Fig. 5C), the data indicate the important role of integrin in interface force transmission between cells and the matrix hydrogel.

Discussion

In the past decade, cell mechanical communication in the large spatial scale has been increasingly recognized. In epithelial collective migration on hard substrates, cell mechanical communications through cell-cell junctional connections have been identified[33,34]. However, the role of traction forces transmitted over the matrix environment is still to be determined during cell collective migration, which would more mimic in vivo soft-tissue condition surrounded by extracellular matrix. From our recent experimental model, cells are able to sense traction transmitted through the matrix to induce mechanical communication over long distances, resulting in cell directed protrusion, migration, and connectivity[57]. Hence, traction force transmitted via the matrix was studied in cell collective migration in this work.

ERK activity is sensitive to cell mechanical stimulus, so the renal epithelial MDCK cells stably expressing ERK FRET biosensor provided a chance to indicate cell mechanical microenvironment and mechano-response. Two types of bioactive materials derived from in vivo were applied as nonlinear elastic hydrogels: Matrigel assembles into reticular network structure to mimic basement membrane, and type I collagen forms fibers to facilitate force transmission efficiency[65,66]. ERK had higher activity at the front of MDCK monolayer migration on Mat + COL hydrogel, of which also showed higher activity than only Mat or Gluta-fixed one (Fig. 1B-C). Previous work also demonstrated higher ERK activity at the front of MDCK collective migration on hard substrate[34], together

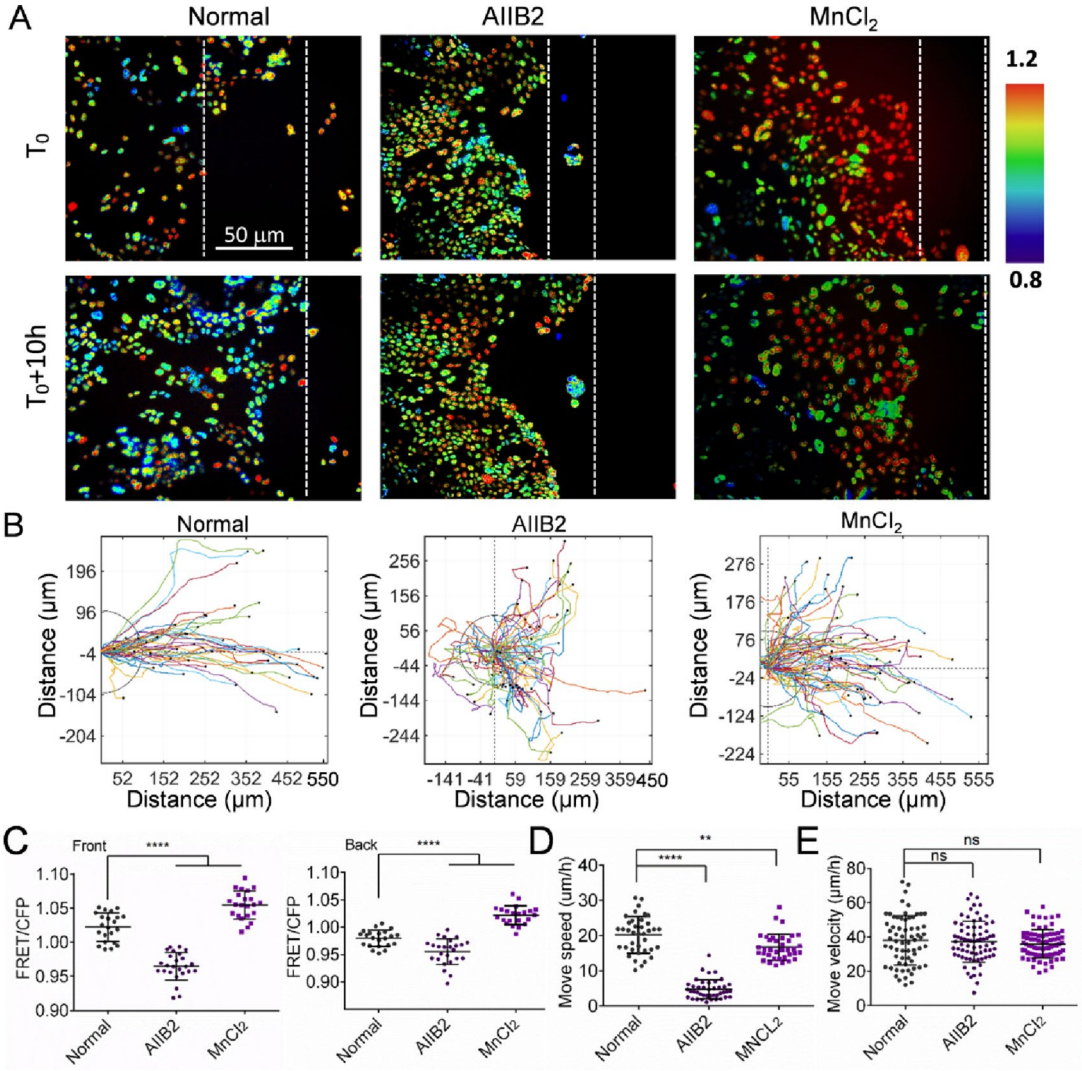

Fig. 5. The integrin pathway in regulating epithelial migration. MDCK cells were seeded on Mat + COL hydrogel cocultured with AIIB2 antibody or $MnCl_2$. **(A)** Representative ERK FRET images for cell collective migrations within 10 h under the three conditions. **(B)** ERK FRET comparisons between the indicated conditions. **(C)** Statistical comparisons of cell moving speeds and velocities for the indicated three conditions. $n = 36, 44, 38$ (speed), and 65, 74, 77 (velocity), respectively. **(D)** Trajectory analysis of individual cells within 10 h for the three conditions. **(E)** Cell viability assay by CCK-8 kit for incubations with the different reagents.

indicating gradient force distribution in the epithelial sheet migration. The mechanosensitive ERK activity was in consistent trend with the monolayer migration speed (Fig. 1D-E), which suggests higher tension force on the Mat + COL hydrogel.

From beads tracking assay, the relative traction force evaluations on the three hydrogel conditions (Fig. 2A-B) showed consistency with monolayer moving speeds and ERK activities. The beads moved forward in the same direction of the collective monolayer migration, which indicates that the matrix traction force was mostly generated from the front cell group and propagated toward the migration direction, resulting in a pulling effect on the hydrogel. Consistently, mechanosensitive ERK showed higher activity at the migration front than at the back (Fig. 1B). As control without substrate traction transmission, cells seeding on the coated matrix (Mat + COL and only Mat) didn't show obvious difference in ERK and collective migration (Fig. S1B-D). These results support the role of traction force transmission via matrix in promoting epithelial collective migration, although the ECM self is necessary in integrin activation and collective migration.

The measured mechanical properties in Fig. 2C didn't change our major conclusion that traction force transmission via the hydrogel matrix promotes the collective migration. Gluta-fixation enhanced the hydrogel stiffness which would speed up cell migration, whereas collective migration was much inhibited due to inhibited traction force transmission after fixation. Matrigel only had a little lower stiffness than Mat + COL one, and the bead traction assays indicated lower traction force on Matrigel only along with lower migration, so it supports the major conclusion as well. As a worthy note, dynamic traction force transmission via matrix is the main point in this experimental model, instead of the static traction force generated from local cell contractions.

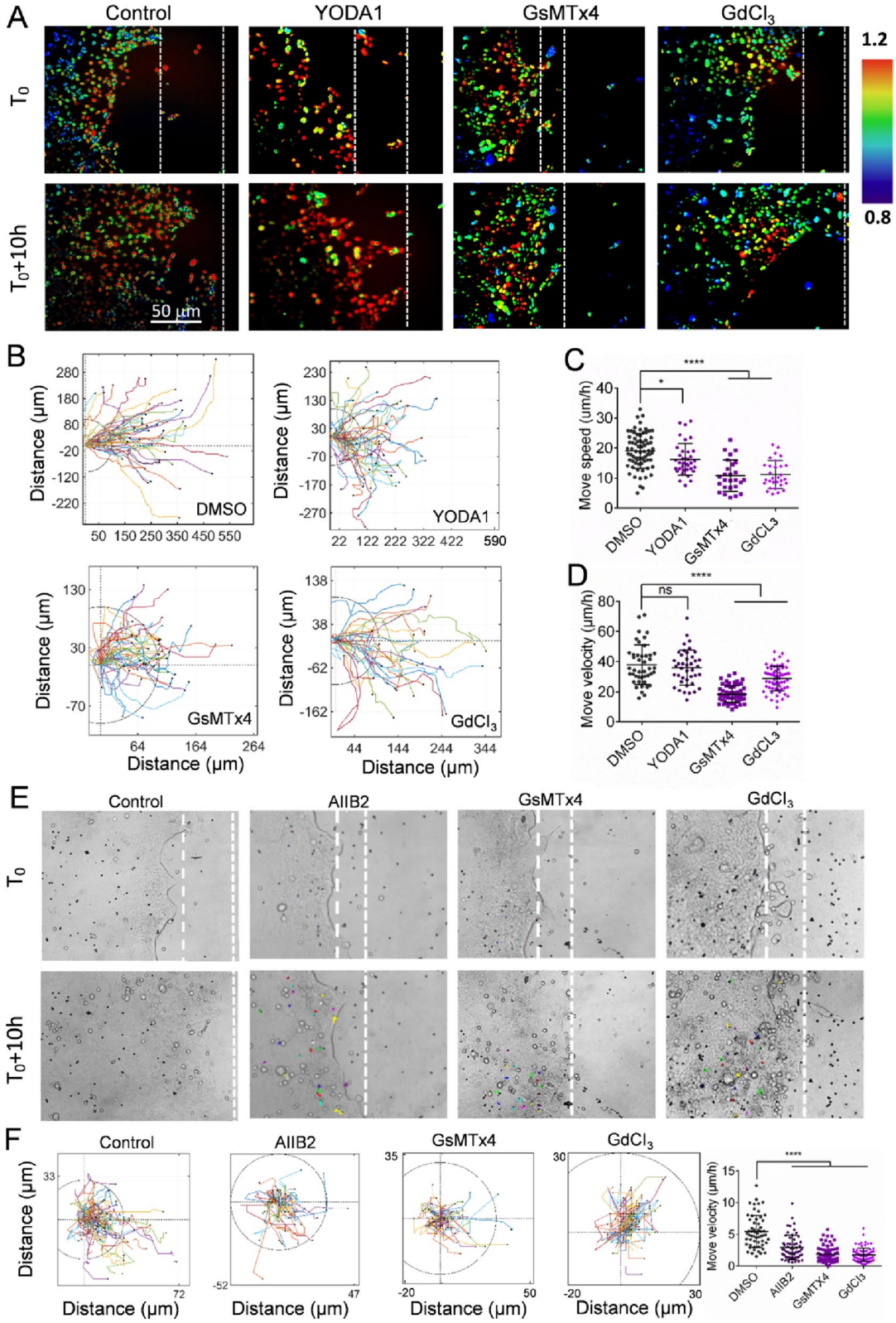

Fig. 6. Piezo1 in regulating epithelial migration and matrix traction force assays. MDCK cells were seeded on Mat + COL hydrogel cocultured with Piezo1 activator YODA1, or inhibitor GsMTx4 or $GdCl_3$. **(A)** Representative ERK FRET images for the indicated conditions during cell collective migrations. **(B-D)** Trajectory analysis of individual cells (B) and statistical comparisons of cell moving speeds/velocities (C, D) within 10 h for the indicated conditions. $n = 73, 36, 26, 30$ (speed), and 45, 41, 59, 66 (velocity), respectively. **(E)** Time-lapse brightfield images of cell monolayer migrations along with black magnetic beads embedded in the hydrogels when cocultured with integrin or Piezo1 inhibitor. **(F)** Trajectory analysis of individual beads and their moving rate comparison at the front groups in 10 h.

Next, the hypothetic mechanism was examined to investigate how matrix tension force is generated and promotes the epithelial monolayer migration. ERK inhibition reduced the collective migration (Fig. 3A-B), similarly to the decreased ERK and migration on Gluta-fixed hydrogel without traction transmission (Figs. 1C-D, and 2F). This indicates ERK importance in the epithelial sheet migration, consistently with previous work, whereas the reported ERK wave wasn't observed in our matrix hydrogel model[34,37,67]. As one reasonable explanation, the force transmission on hard substrate was mainly via cell junctions-based epithelial sheet, which stimulated ERK activation waves, whereas on the matrix hydrogel, force transmission was mainly via the matrix, hence ERK wave was not obvious.

Hypothetically, the matrix traction force was derived from cells-generated contractions. Inhibition of cell contractive force reduced both ERK activity and collective migration (Fig. 4B-C), which was consistent with matrix traction force derived from cell contractions. Integrin is the major force transducer at the interface between cells and the matrix. Interestingly, blocking integrin activation by β1 AIIB2 antibody inhibited ERK, matrix traction force, and collective migration, but not local cell moving velocity (indicating normal intracellular activities) (Figs. 5B-C, and 6F), which suggests the mechanotransduction role of integrin in force transmission between cells and matrix to orientate the migration direction. These data together indicate that cell contraction force was transmitted into the matrix which traction force transmission stimulated epithelial sheet migration as feedback.

To further explore mechanobiological mechanism for matrix traction-stimulated epithelial collective migration, calcium channels on plasma membrane and endoplasmic reticulum, and Piezo1 channels were checked in the experimental model. Inhibitions of these mechanosensitive channels reduced epithelial migration (Figs. S2B-C, and 6B-D). It was confirmed that Piezo1 inhibition led to matrix traction reduction (Fig. 6F). These data implicate that these mechanosensitive calcium channels are relevant to the traction force-stimulated epithelial sheet migration. It is noted that the results are considered as supportive only at this stage since inhibitions of these essential ion channels might also interfere with cellular normal functions.

This in vitro cell culture model revealed certain principle in traction force-promoting collective migration via the hydrogel transmission. As the implications in vivo, cells or tissues generally grow on extracellular matrix, and hypothetically, the traction force from cells could be transmitted via the matrix components to build cell-cell mechanical communications, such as for maintaining tissue homeostasis, collective migration, synchronized cardiomyocyte beating. In pathologies, the matrix traction force transmission could also facilitate the metastasis of cancer cells which often move collectively, and the progress of fibrosis within tissues.

Conclusion

In a conclusion model (as depicted on illustrated Fig. 7), matrix traction force is derived from cells-generated contraction, of which integrin acts with necessary mechanotransduction role at the interface between cells and the hydrogel; the tension force transmitted over the hydrogel promotes the epithelial collective migration, which relies on activations of cell mechanosensitive calcium channels (including Piezo1), and ERK signals; cross-linking of the hydrogel by glutaraldehyde blocks matrix tension force transmission and then reduces the collective migration efficiency. This work highlights the role of matrix traction force in wound healing processes and tissue regenerations.

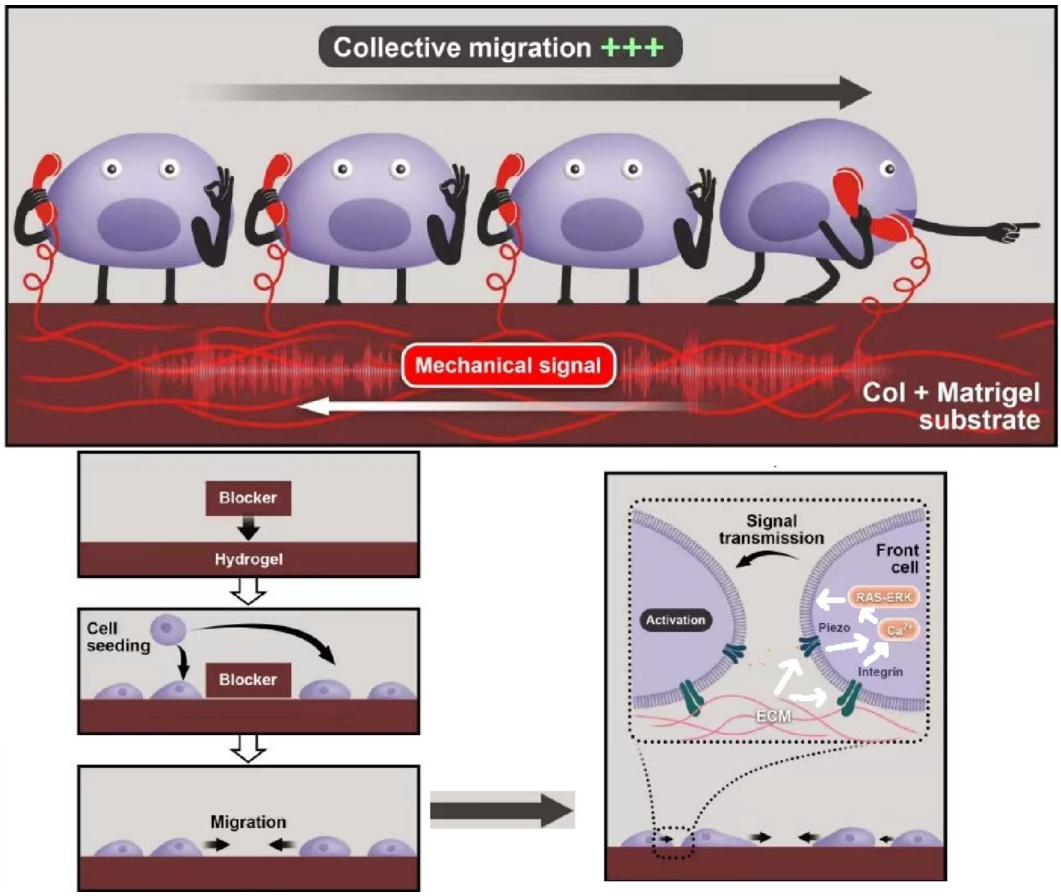

Fig. 7. Matrix traction force-promoted epithelial collective migration. The conclusion model (top panel): matrix traction force is derived from cells contraction, of which integrin acts with necessary mechanotransduction role between cells and the hydrogel; the tension force over the hydrogel promotes the epithelial collective migration, which relies on activations of cellular calcium and Piezo1 channels, and ERK signals. **The experimental setups (below panel)**: the matrix hydrogel containing 50% Matrigel and 1 mg/mL type I collagen is confined by PDMS mold (1 cm in diameter), and a cubic blocker of 4% agarose gel is placed on the center of hydrogel surface, followed by seeding MDCK cells on the rest hydrogel surface; after the cells grow into confluency, the blocking area is gently lifted, and the epithelial sheet migrates towards the blank area collectively, of which is regulated by mechanosensitive signaling pathways (indicating of intermolecular relations by the arrows).

Data availability

The datasets used and/or analysed during the current study available from the corresponding author on reasonable request.

Received: 17 November 2025; Accepted: 2 February 2026
Published online: 18 February 2026

References

1. Guo, C. L. et al. Long-range mechanical force enables self-assembly of epithelial tubular patterns. *Proc. Natl. Acad. Sci. U S A.* **109**, 5576–5582. https://doi.org/10.1073/pnas.1114781109 (2012).
2. Shi, Q. et al. Rapid disorganization of mechanically interacting systems of mammary acini. *Proc. Natl. Acad. Sci. U S A.* **111**, 658–663. https://doi.org/10.1073/pnas.1311312110 (2014).
3. Sapir, L. & Tzlil, S. Talking over the extracellular matrix: how do cells communicate mechanically? *Semin Cell. Dev. Biol.* **71**, 99–105. https://doi.org/10.1016/j.semcdb.2017.06.010 (2017).
4. Alisafaei, F., Chen, X., Leahy, T., Janmey, P. A. & Shenoy, V. B. Long-range mechanical signaling in biological systems. *Soft Matter.* **17**, 241–253. https://doi.org/10.1039/d0sm01442g (2021).
5. Long, Y., Niu, Y., Liang, K. & Du, Y. Mechanical communication in fibrosis progression. *Trends Cell. Biol.* **32**, 70–90. https://doi.org/10.1016/j.tcb.2021.10.002 (2022).
6. Pakshir, P. et al. Dynamic fibroblast contractions attract remote macrophages in fibrillar collagen matrix. *Nat. Commun.* **10**, 1850. https://doi.org/10.1038/s41467-019-09709-6 (2019).
7. Ouyang, M. et al. The underlying difference of metastatic and non-metastatic breast cancer cells in configuring type I collagen fibres to promote migration by cell mechanics. *Mechanobiol. Med.* **3**, 100113. https://doi.org/10.1016/j.mbm.2025.100113 (2025).

8. Wang, H., Abhilash, A. S., Chen, C. S., Wells, R. G. & Shenoy, V. B. Long-range force transmission in fibrous matrices enabled by tension-driven alignment of fibers. *Biophys. J.* **107**, 2592–2603. https://doi.org/10.1016/j.bpj.2014.09.044 (2014).
9. Hall, M. S. et al. Fibrous nonlinear elasticity enables positive mechanical feedback between cells and ECMs. *Proc. Natl. Acad. Sci. U S A.* **113**, 14043–14048. https://doi.org/10.1073/pnas.1613058113 (2016).
10. Ouyang, M. et al. Cell mechanics regulates the dynamic anisotropic remodeling of fibril matrix at large scale. *Res. (Wash D C.* **6**, 0270. https://doi.org/10.34133/research.0270 (2023).
11. Fan, Q. et al. Dynamically Re-Organized collagen fiber bundles transmit mechanical signals and induce strongly correlated cell migration and Self-Organization. *Angew Chem. Int. Ed. Engl.* **60**, 11858–11867. https://doi.org/10.1002/anie.202016084 (2021).
12. Abhilash, A. S., Baker, B. M., Trappmann, B., Chen, C. S. & Shenoy, V. B. Remodeling of fibrous extracellular matrices by contractile cells: predictions from discrete fiber network simulations. *Biophys. J.* **107**, 1829–1840. https://doi.org/10.1016/j.bpj.2014.08.029 (2014).
13. Lin, J. Y., Lo, K. Y. & Sun, Y. S. A microfluidics-based wound-healing assay for studying the effects of shear stresses, wound widths, and chemicals on the wound-healing process. *Sci. Rep.* **9**, 20016. https://doi.org/10.1038/s41598-019-56753-9 (2019).
14. Xue, J., Wu, T., Xia, Y. & Perspective Aligned arrays of electrospun nanofibers for directing cell migration. *APL Mater.* **6** https://doi.org/10.1063/1.5058083 (2018).
15. Lee, R. M., Kelley, D. H., Nordstrom, K. N., Ouellette, N. T. & Losert, W. Quantifying stretching and rearrangement in epithelial sheet migration. *New. J. Phys.* **15** https://doi.org/10.1088/1367-2630/15/2/025036 (2013).
16. Yu, P., Li, Y., Fang, W., Feng, X. Q. & Li, B. Mechanochemical dynamics of collective cells and hierarchical topological defects in multicellular lumens. *Sci. Adv.* **10**, eadn0172. https://doi.org/10.1126/sciadv.adn0172 (2024).
17. Hakkinen, H. M., Villaseca, S., De La Burgade, M., Alhashem, Z. & Scarpa, E. Collective migration in complex environments: the case of the trunk neural crest. *Curr. Top. Dev. Biol.* **164**, 109–151. https://doi.org/10.1016/bs.ctdb.2025.01.004 (2025).
18. Clark, A. G. et al. Self-generated gradients steer collective migration on viscoelastic collagen networks. *Nat. Mater.* **21**, 1200–1210. https://doi.org/10.1038/s41563-022-01259-5 (2022).
19. Sun, J., Macabenta, F., Akos, Z. & Stathopoulos, A. Collective migrations of drosophila embryonic trunk and caudal Mesoderm-Derived muscle precursor cells. *Genetics* **215**, 297–322. https://doi.org/10.1534/genetics.120.303258 (2020).
20. Lu, W. & Kang, Y. Epithelial-Mesenchymal plasticity in cancer progression and metastasis. *Dev. Cell.* **49**, 361–374. https://doi.org/10.1016/j.devcel.2019.04.010 (2019).
21. Riahi, R., Yang, Y., Zhang, D. D. & Wong, P. K. Advances in Wound-Healing assays for probing collective cell migration. *J. Lab. Autom.* **17**, 59–65 (2012).
22. Yamaguchi, N., Mizutani, T., Kawabata, K. & Haga, H. Leader cells regulate collective cell migration via Rac activation in the downstream signaling of integrin β1 and PI3K. *Sci. Rep.* **5**, 7656. https://doi.org/10.1038/srep07656 (2015).
23. Ratheesh, A., Belyaeva, V. & Siekhaus, D. E. Drosophila immune cell migration and adhesion during embryonic development and larval immune responses. *Curr. Opin. Cell Biol.* **36**, 71–79 (2015).
24. Stepien, T. L., Lynch, H. E., Yancey, S. X., Dempsey, L. & Davidson, L. A. Using a continuum model to Decipher the mechanics of embryonic tissue spreading from time-lapse image sequences: an approximate bayesian computation approach. *PLoS One.* **14**, e0218021. https://doi.org/10.1371/journal.pone.0218021 (2019).
25. Raftopoulou, M. & Hall, A. Cell migration: Rho GTPases lead the way. *Dev. Biol.* **265**, 23–32. https://doi.org/10.1016/j.ydbio.2003.06.003 (2004).
26. Margiotta, A. & Bucci, C. Coordination between Rac1 and Rab Proteins: Functional Implications in Health and Disease. *Cells* **8**, (2019). https://doi.org/10.3390/cells8050396
27. Lin, S. et al. Redundant roles of EGFR ligands in the ERK activation waves during collective cell migration. *Life Sci. Alliance.* **5** https://doi.org/10.26508/lsa.202101206 (2022).
28. Reffay, M. et al. Interplay of RhoA and mechanical forces in collective cell migration driven by leader cells. *Nat. Cell. Biol.* **16**, 217–223. https://doi.org/10.1038/ncb2917 (2014).
29. Das, T. et al. A molecular mechanotransduction pathway regulates collective migration of epithelial cells. *Nat. Cell Biol.* **17**, 276–287. https://doi.org/10.1038/ncb3115 (2015).
30. Dukes, J. D., Whitley, P. & Chalmers, A. D. The MDCK variety pack: choosing the right strain. *BMC Cell. Biol.* **12**, 43. https://doi.org/10.1186/1471-2121-12-43 (2011).
31. Ladoux, B. & Mège, R. M. Mechanobiology of collective cell behaviours. *Nat. Rev. Mol. Cell. Biol.* **18**, 743–757. https://doi.org/10.1038/nrm.2017.98 (2017).
32. Vining, K. H. & Mooney, D. J. Mechanical forces direct stem cell behaviour in development and regeneration. *Nat. Rev. Mol. Cell. Biol.* **18**, 728–742. https://doi.org/10.1038/nrm.2017.108 (2017).
33. Sunyer, R. et al. Collective cell durotaxis emerges from long-range intercellular force transmission. *Science* **353**, 1157–1161. https://doi.org/10.1126/science.aaf7119 (2016).
34. Hino, N. et al. ERK-Mediated mechanochemical waves direct collective cell polarization. *Dev. Cell.* **53**, 646–660e648. https://doi.org/10.1016/j.devcel.2020.05.011 (2020).
35. Shellard, A., Szabó, A., Trepat, X. & Mayor, R. Supracellular contraction at the Rear of neural crest cell groups drives collective chemotaxis. *Science* **362**, 339–343. https://doi.org/10.1126/science.aau3301 (2018).
36. Shellard, A. & Mayor, R. Collective durotaxis along a self-generated stiffness gradient in vivo. *Nature* **600**, 690–694. https://doi.org/10.1038/s41586-021-04210-x (2021).
37. Hino, N. et al. A feedback loop between lamellipodial extension and HGF-ERK signaling specifies leader cells during collective cell migration. *Dev. Cell.* **57**, 2290–2304e2297. https://doi.org/10.1016/j.devcel.2022.09.003 (2022).
38. Gilmour, A., Poole-Warren, L. & Green, R. A. An improved in vitro model of cortical tissue. *Front. Neurosci.* **13**, 1349. https://doi.org/10.3389/fnins.2019.01349 (2019).
39. Liu, Q. P., Luo, Q., Deng, B., Ju, Y. & Song, G. B. Stiffer matrix accelerates migration of hepatocellular carcinoma cells through enhanced aerobic Glycolysis via the MAPK-YAP signaling. *Cancers (Basel).* **12** https://doi.org/10.3390/cancers12020490 (2020).
40. Bai, H., Yang, J., Meng, S. & Liu, C. Oral Microbiota-Driven cell migration in carcinogenesis and metastasis. *Front. Cell. Infect. Microbiol.* **12**, 864479. https://doi.org/10.3389/fcimb.2022.864479 (2022).
41. Pham, H. L. et al. PDMS micropatterns coated with PDA and RGD induce a regulatory Macrophage-like phenotype. *Micromachines (Basel).* 14. https://doi.org/10.3390/mi14030673 (2023).
42. Wang, X. et al. Piezo type mechanosensitive ion channel component 1 facilitates gastric cancer omentum metastasis. *J. Cell. Mol. Med.* **25**, 2238–2253. https://doi.org/10.1111/jcmm.16217 (2021).
43. Zhang, G., Li, X., Wu, L. & Qin, Y. X. Piezo1 channel activation in response to Mechanobiological acoustic radiation force in osteoblastic cells. *Bone Res.* **9**, 16. https://doi.org/10.1038/s41413-020-00124-y (2021).
44. Xiong, Y. et al. Piezo1 activation facilitates ovarian cancer metastasis via Hippo/YAP signaling axis. *Channels (Austin).* **16**, 159–166. https://doi.org/10.1080/19336950.2022.2099381 (2022).
45. Ouyang, M. et al. Mechanical communication-associated cell directional migration and branching connections mediated by calcium channels, integrin β1, and N-cadherin. *Front. Cell. Dev. Biol.* **10**, 942058. https://doi.org/10.3389/fcell.2022.942058 (2022).
46. Ouyang, M. et al. alpha-Catenin and Piezo1 mediate cell mechanical communication via cell adhesions. *Biology (Basel).* **13**. https://doi.org/10.3390/biology13050357 (2024).
47. Zhang, Y. et al. Mechanical stress facilitates calcium influx and growth of alveolar epithelial cells via activation of the BDKRB1/Ca(2+)/CaMKII/MEK1/ERK axis. *Respir Res.* **26**, 168. https://doi.org/10.1186/s12931-025-03240-7 (2025).

48. Fang, X. et al. FRET visualization of Cyclic Stretch-Activated ERK via calcium channels mechanosensation while not integrin β1 in airway smooth muscle cells. *Front. Cell. Dev. Biol.* **10**, 847852. https://doi.org/10.3389/fcell.2022.847852 (2022).
49. Rasl, J. et al. ERK2 signaling regulates cell-cell adhesion of epithelial cells and enhances growth factor-induced cell scattering. *Cell. Signal.* **99**, 110431. https://doi.org/10.1016/j.cellsig.2022.110431 (2022).
50. Komatsu, N. et al. Development of an optimized backbone of FRET biosensors for kinases and GTPases. *Mol. Biol. Cell.* **22**, 4647–4656. https://doi.org/10.1091/mbc.E11-01-0072 (2011).
51. Iroegbu, J. D., Ijomone, O. K., Femi-Akinlosotu, O. M. & Ijomone, O. M. ERK/MAPK signalling in the developing brain: perturbations and consequences. *Neurosci. Biobehav Rev.* **131**, 792–805. https://doi.org/10.1016/j.neubiorev.2021.10.009 (2021).
52. Wu, P. K., Becker, A. & Park, J. I. Growth inhibitory signaling of the Raf/MEK/ERK pathway. *Int. J. Mol. Sci.* **21** https://doi.org/10.3390/ijms21155436 (2020).
53. Harvey, C. D. et al. A genetically encoded fluorescent sensor of ERK activity. *Proc. Natl. Acad. Sci. U S A.* **105**, 19264–19269. https://doi.org/10.1073/pnas.0804598105 (2008).
54. Aoki, K. et al. Propagating wave of ERK activation orients collective cell migration. *Dev. Cell.* **43**, 305–317e305. https://doi.org/10.1016/j.devcel.2017.10.016 (2017).
55. Hiratsuka, T. et al. Intercellular propagation of extracellular signal-regulated kinase activation revealed by in vivo imaging of mouse skin. *Elife* **4**, e05178. https://doi.org/10.7554/eLife.05178 (2015).
56. Boocock, D., Hino, N., Ruzickova, N., Hirashima, T. & Hannezo, E. Theory of mechanochemical patterning and optimal migration in cell monolayers. *Nat. Phys.* **17**, 267–274. https://doi.org/10.1038/s41567-020-01037-7 (2021).
57. Ouyang, M. et al. Sensing traction force on the matrix induces Cell-Cell distant mechanical communications for Self-Assembly. *ACS Biomater. Sci. Eng.* **6**, 5833–5848. https://doi.org/10.1021/acsbiomaterials.0c01035 (2020).
58. Zhong, J. Y. et al. Fe2O3 nanoparticles disrupt microstructure and reduce the viscoelasticity of simulated asthma airway mucus for potential airway mucus clearance applications. *Front. Physiol.* **16** https://doi.org/10.3389/fphys.2025.1566716 (2025).
59. Qin, Q. et al. Fluocell for ratiometric and High-Throughput Live-Cell image visualization and quantitation. *Front. Phys.* **7** https://doi.org/10.3389/fphy.2019.00154 (2019).
60. Chen, Y., Dodd, S. J., Tangrea, M. A., Emmert-Buck, M. R. & Koretsky, A. P. Measuring collective cell movement and extracellular matrix interactions using magnetic resonance imaging. *Sci. Rep.* **3**, 1879. https://doi.org/10.1038/srep01879 (2013).
61. Kim, T. J. et al. Distinct mechanisms regulating mechanical force-induced Ca(2)(+) signals at the plasma membrane and the ER in human MSCs. *Elife* **4**, e04876. https://doi.org/10.7554/eLife.04876 (2015).
62. Xu, S. et al. Integrin-α9β1 as a novel therapeutic target for refractory diseases: recent progress and insights. *Front. Immunol.* **12**, 638400. https://doi.org/10.3389/fimmu.2021.638400 (2021).
63. Tiwari, S., Askari, J. A., Humphries, M. J. & Bulleid, N. J. Divalent cations regulate the folding and activation status of integrins during their intracellular trafficking. *J. Cell. Sci.* **124**, 1672–1680. https://doi.org/10.1242/jcs.084483 (2011).
64. Lai, A. et al. Mechanosensing by Piezo1 and its implications for physiology and various pathologies. *Biol. Rev. Camb. Philos. Soc.* **97**, 604–614. https://doi.org/10.1111/brv.12814 (2022).
65. Poincloux, R., Lizarraga, F. & Chavrier, P. Matrix invasion by tumour cells: a focus on MT1-MMP trafficking to invadopodia. *J. Cell. Sci.* **122**, 3015–3024. https://doi.org/10.1242/jcs.034561 (2009).
66. Bagchi, A., Sarker, B., Zhang, J., Foston, M. & Pathak, A. Fast yet force-effective mode of supracellular collective cell migration due to extracellular force transmission. *PLoS Comput. Biol.* **21**, e1012664. https://doi.org/10.1371/journal.pcbi.1012664 (2025).
67. Samson, S. C., Khan, A. M. & Mendoza, M. C. ERK signaling for cell migration and invasion. *Front. Mol. Biosci.* **9**, 998475. https://doi.org/10.3389/fmolb.2022.998475 (2022).

Acknowledgements

The experiments were assisted by lab technicians Yan Pan, and Jingjing Li (Changzhou University). The cartoon Figure 7 was illustrated by Dr. Yang Jin (Chongqing University).

Author contributions

Y.C. performed the major experiments and data analysis; M.O., Y.C. and L.D. designed the experiments and carried the data organization; H.S., H.L., L.L., C.L. and B.B. provided technical helps and discussion; L.D. provided the setups of equipment; M.O., Y.C. and L.D. prepared the manuscript.

Funding

This work was funded by National Natural Science Foundation of China (NSFC 12372312), and Project of "Jiangsu Specially-appointed Professor" (M.O.); National Natural Science Foundation of China (NSFC 12272063) (L.D.).

Declarations

Competing interests

The authors declare no competing interests.

Additional information

Supplementary Information The online version contains supplementary material available at https://doi.org/10.1038/s41598-026-39048-8.

Correspondence and requests for materials should be addressed to M.O. or L.D.

Reprints and permissions information is available at www.nature.com/reprints.

Publisher's note Springer Nature remains neutral with regard to jurisdictional claims in published maps and institutional affiliations.